

Analysis of Stress Concentrations in Adhesively-Bonded Assemblies subject to Thermo-Mechanical Loads: Application to the Characterisation of the Adhesive Behaviour

J.Y. Cognard¹, C. Badulescu¹, N. Carrère¹, R. Créac'hcadec¹ and P. Védrine²

¹Laboratoire Brestois de Mécanique et des Systèmes
ENSTA Bretagne/Université de Brest/ENIB/UEB, France

²CEA Saclay, DSM/Irfu/SACM, Gif sur Yvette, France

Abstract

Bonded assemblies are increasingly used in the design of mechanical structures due to major advantages of this technique, i.e. the weight reduction and the facility to join different material and especially composites. But bonded assemblies are often characterized by large stress concentrations at the ends of the overlap length. Moreover, the use of bonded assemblies at different temperatures can lead to an increase of stress concentrations associated with the thermal stresses. Thus, specific studies are required as the mechanical behaviour of the adhesive and the stress concentrations in bounded assemblies can depend on the service temperature, especially in the case of high-tech applications under low temperatures. The coefficients of thermal expansion for the adherents and the adhesive are generally different, thus a change of service temperature lead to a pre-load of the adhesive which can also be associated with stress concentrations. Therefore such properties have to be taken into account in the joint design. The objective of the paper is first to characterize the influence of thermo-mechanical loads on the stress state in a bonded assembly under elastic assumption by taking into account the temperature dependent of the mechanical properties of the adhesive. Such thermo-mechanical loads can lead to complex history path in the von Mises equivalent stress – hydrostatic stress plane which is often used to describe the temperature dependent elastic limit of an adhesive. Starting from two-dimensional numerical simulations, the influence of the service temperature on the stress concentrations is analysed in order to define the requirements of the bonded specimens for reliable experimental tests. Some experimental results, for a temperature range between 20 °C and -60 °C using a modified Arcan device designed to strongly limit stress concentrations, are presented in order to validate the proposed numerical studies.

Keywords: adhesively-bonded joint, stress concentration, thermo-mechanical loads, finite element analysis, joint design.

1 Introduction

Bonded assemblies are increasingly used in the design of mechanical structures due to major advantages of this technique, i.e. the weight reduction and the facility to join different material and especially composites [1-3]. But bonded assemblies are often characterized by large stress concentrations at the ends of the overlap length which are mainly associated with a high ratio of the mechanical properties between the adhesive and the adherent, the low thickness of the adhesive in the assembly and the mechanical load [4-5]. Moreover, the use of bonded assemblies at different temperatures [6] can lead to an increase of the stress concentrations associated with the thermal stresses [7-8]. Thus, specific studies are required as the mechanical behaviour of the adhesive and the stress concentrations in bounded assemblies can depend on the service temperature, especially in the case of high-tech applications under high or low temperatures. The Young modulus and the so-called elastic limit of an adhesive strongly depend on the service temperature. Moreover, the coefficients of thermal expansion for the adherents and the adhesive are generally different, thus a change of service temperature lead to a pre-load of the adhesive which can also be associated with stress concentrations. Therefore such properties have to be taken into account in the joint design.

Bulk, lap-shear and pull-off tests are often used to analyse the mechanical behaviour of adhesives [9]. Such experiments give information about the mechanical behaviour of the adhesive but the influence of defects and the influence of stress concentrations are often difficult to take into account. Moreover, in order to model the complex behaviour of adhesives in assemblies, non associated pressure-dependent constitutive models have to be used [10]. The identification of the material parameters of such models requires a large data base of experimental results under various compression/tensile-shear tests and a precise analysis of the non-linear behaviour of the adhesive. Therefore, it is interesting to analyse the possibilities of the modified Arcan device developed to strongly limit the stress concentrations and used mainly at present time at room temperature [11], in order to determine, at different temperatures, the behaviour of adhesives in an assembly. The stress singularities can contribute to the initiation of fracture in adhesive joints and thus lead to an incorrect analysis of the behaviour of the adhesive. Therefore, understanding the stress distribution in an adhesive joint can lead to improvements in adhesively-bonded assemblies.

The objective of the paper is first to characterize the influence of thermo-mechanical loads on the stress state in a bonded assembly under elastic assumption. Such thermo-mechanical loads can lead to complex history path in the von Mises equivalent stress – hydrostatic stress plane which is often used to describe the temperature dependent elastic limit of an adhesive. Starting from 2D numerical simulations, the influence of the service temperature on the stress concentrations is analysed in order to define the requirements of the bonded specimens for reliable experimental tests. Some experimental results, for a temperature range between 20 °C and -60 °C using a modified Arcan device designed to strongly limit stress concentrations, are presented in order to validate the proposed numerical studies.

2 Experimental device

In a previous project, in order to be able to study accurately the behavior of an adhesive in an assembly as a function of the normal stress component and to use a traditional tensile testing machine, a modified Arcan fixture [12] was developed, which enabled compression or tension to be combined with shear loads.

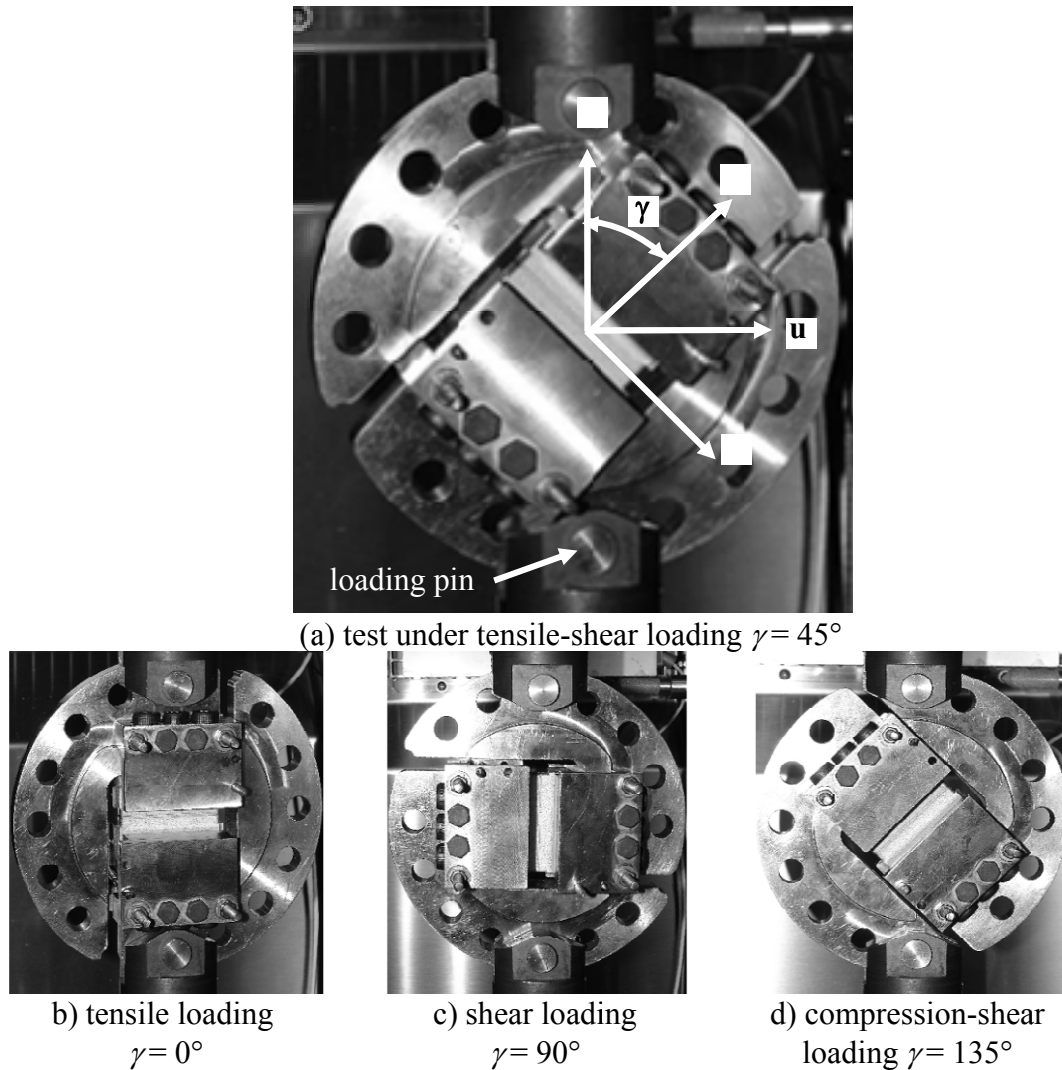


Figure 1: Modified Arcan device.

Figure 1 presents the modified Arcan device; the orientation between the loading direction and the mean plane of the adhesive is defined by the angle γ . For tension tests: γ is equal to 0° (Figure 1); for tensile-shear tests with the same load in tension and shear: $\gamma = 45^\circ$; for shear tests: $\gamma = 90^\circ$ and for compression-shear tests with the same load in tension and shear: $\gamma = 135^\circ$. Other directions can be used. Numerical simulations under linear elasticity assumption, for bi-material structures show that

the use of a special geometry for the substrate (a beak close to the adhesive joint) strongly reduces the stress concentrations due to edge effects [11] (Figure 2), which are mainly associated with a high ratio of the mechanical properties between the adhesive and the adherents (mainly the Young modulus) and the low thickness of the adhesive in the assembly. Moreover the system fixing the substrates on the supporting Arcan fixture was designed in order to prevent pre-loading of the specimen [11, 12].

To ensure a precise adhesive thickness and a good relative positioning of the two substrates during the bonding process, spacers are manufactured during the machining process of the substrates (Figure 2). It can be noted in Figure 2 that beaks are machined all around the substrates close to the bonded area and a cleaning of the free edges of the adhesive is performed before the curing process in order to limit stress concentrations in the case of structural adhesives [11]. Screws are used to ensure the relative positioning of the two substrates during the bonding process; moreover, a torque of 2.5 mN is applied with a screwdriver to limit the scatter in the adhesive thickness [13]. After the curing process, the spacers are cut to obtain the bonded specimen to be used with the modified Arcan device. For such specimens, the area of the bonded section is 50 mm x 9 mm.

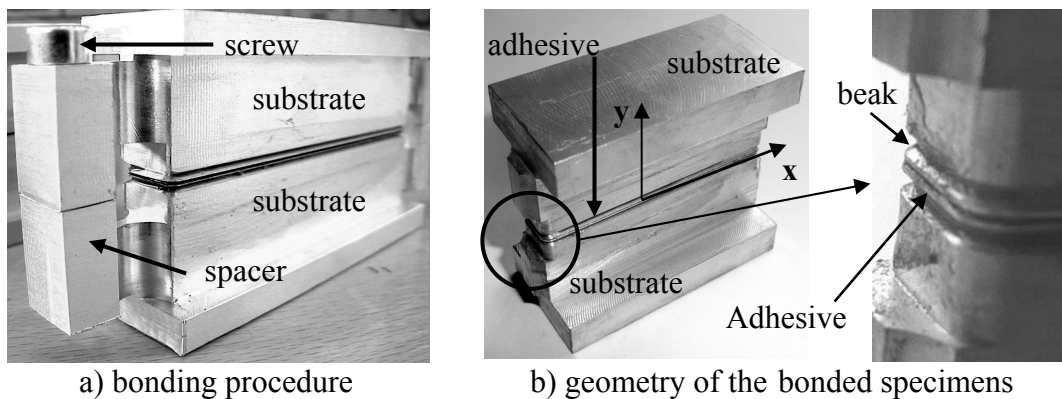


Figure 2: Presentation of the bonded specimens.

Tests were performed using a hydraulic tensile testing machine (Instron), with a maximum load of 100 kN and a thermal chamber (Servatin) available in the laboratory. The thermal chamber has a view-glass which allows us to use an optical 3D measuring system by digital image correlation [14] in order to measure the relative displacement of the two substrates, and thus the deformation of the adhesive, in the x and y directions (Figures 1 and 2) [13]. In the following, DN and DT denote the relative displacements of both ends of the adhesive in the normal (direction x , Figure 1) and tangential directions (direction x , Figure 1). It is important to notice that the displacement measurement through the view-glass of the thermal chamber requires specific adjustments. FN and FT represent the normal and tangential components of the applied load in the normal and tangential directions.

3 Parameters of the numerical simulations

Computations were made in 2D under plane strain assumption. The elastic properties of both materials are: $E_a = 2$ GPa (Young modulus), $\nu_a = 0.3$ (Poisson's ratio) for the adhesive and $E_s = 70$ GPa, $\nu_s = 0.3$ for the substrates. The coefficient of thermal expansion used in this study is equal to $2.3 \text{ E-}5 \text{ }^\circ\text{C}^{-1}$ for the substrate and $8 \text{ E-}5 \text{ }^\circ\text{C}^{-1}$ for the adhesive (value obtained experimentally). Computations were made under plane strain assumption using refined meshes [11]. It can be noted that it is possible to analyse only half of the model using adequate boundary conditions.

In order to correctly determine the way the stress evolves throughout the thickness of the adhesive, precise finite element analyses have to be performed, even assuming a linear elastic behaviour of the components, especially for large material heterogeneity of the assemblies [5, 11]. Moreover refined meshes are also needed near the substrate-adhesive interfaces in order to obtain good numerical results. Various simulations have shown that good numerical results are obtained using meshes with 20 linear rectangular elements for a 0.1 mm thickness of adhesive, especially when stress concentrations are not too large [11]. Moreover, it is important to note that the aim of this study is to analyze specific geometries which significantly limit the influence of edge effects.

Various studies underline that an accurate representation of the elastic yield surface of an adhesive requires the use of a pressure-dependent constitutive model, i.e. a model taking into account the two stress invariants, hydrostatic stress and von Mises equivalent stress. For this study, only elastic behaviour of the adhesive is used. An exponential Drucker-Prager yield function allows a good representation of the experimental data for the so-called ‘‘initial elastic limit’’ [13]:

$$F_0 = a(T) \cdot (\sigma_{vm})^{b(T)} + P_h - P_{h0}(T) = 0$$

Where σ_{vm} is the equivalent von Mises stress and P_h is the hydrostatic stress. a , b and P_{h0} are material parameters. The temperature evolution of the material parameters are such that:

$$\begin{aligned} a(T) &= C_1 \cdot T + D_1 \\ b(T) &= C_2 \cdot T + D_2 \\ P_{h0}(T) &= C_3 \cdot T + D_3 \end{aligned}$$

C_1 (SI units)	C_2 ($^\circ\text{C}$)	C_3 (MPa/ $^\circ\text{C}$)	D_1 (SI units)	D_2	D_3 (MPa)
-1.65 E-6	9.43 E-4	-0.62	1.35 E-4	3.1	41.32

Table 1. Material parameters for the initial yield surface in the hydrostatic pressure-von Mises stress diagram

The results of the identification are presented in Table 1. A good representation of the experimental results is obtained using such type of model [15].

These results have been obtained using the epoxy resin Huntsman™ Araldite 420 A/B with a joint thickness of 0.2 mm [15]. The bonding procedure adopted starts with an immersion of the machined substrates in acetone for three hours to eliminate any presence of cooling oil used in the machining process, which will undoubtedly affect the bonding. After that, surfaces are prepared with sandpaper (grade of 180) to remove any impurities and oxide layer that can potentially exist; moreover, the associated roughness increases the adhesion. A degreasing and cleaning of the surface is accomplished to remove any particles that may remain after sanding. The curing process used is: 1 hour at 110 ° C. The different tests were made with a displacement rate of the crosshead of the tensile testing machine of 0.5 mm/minute.

4 Analysis of stress concentrations in bonded assemblies under thermo-mechanical loads

Bonded assemblies are often characterized by large stress concentrations at the ends of the overlap length which are mainly associated with a high ratio of the mechanical properties between the adhesive and the adherents (mainly the Young modulus), the low thickness of the adhesive in the assembly and the mechanical load [4, 11]. Moreover, the use of bonded assemblies at different temperatures [6] can lead to an increase in the stress concentration associated with the thermal stresses [7-8]. Thus, specific studies are required as the mechanical behaviour of the adhesive and the stress concentrations in bonded assemblies can depend on the service temperature.

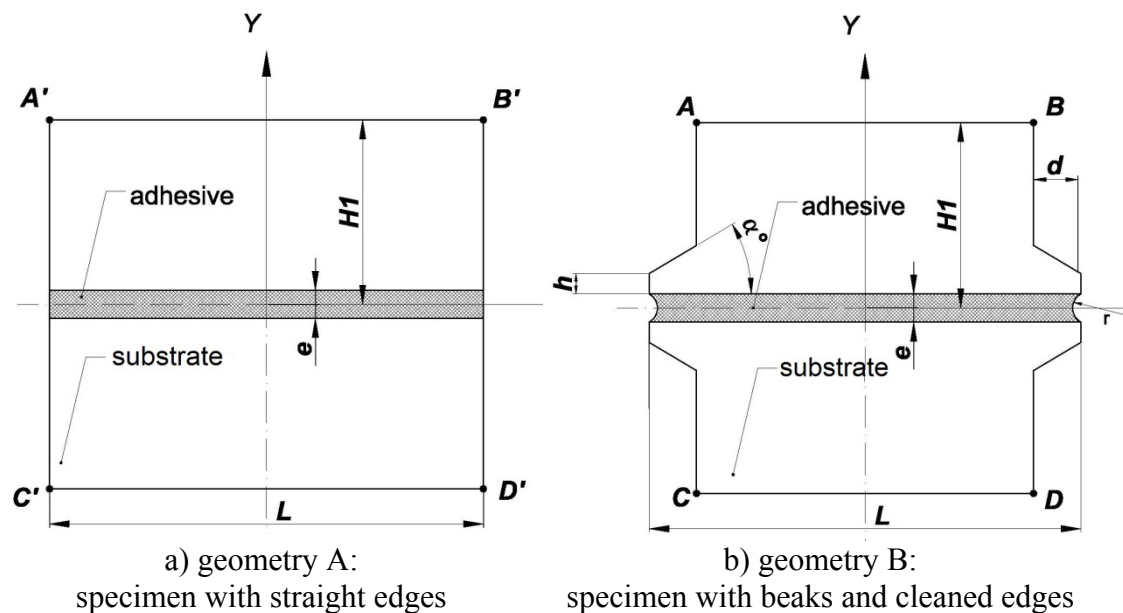


Figure 3: Presentation of two geometries of the bonded assemblies (not to scale).

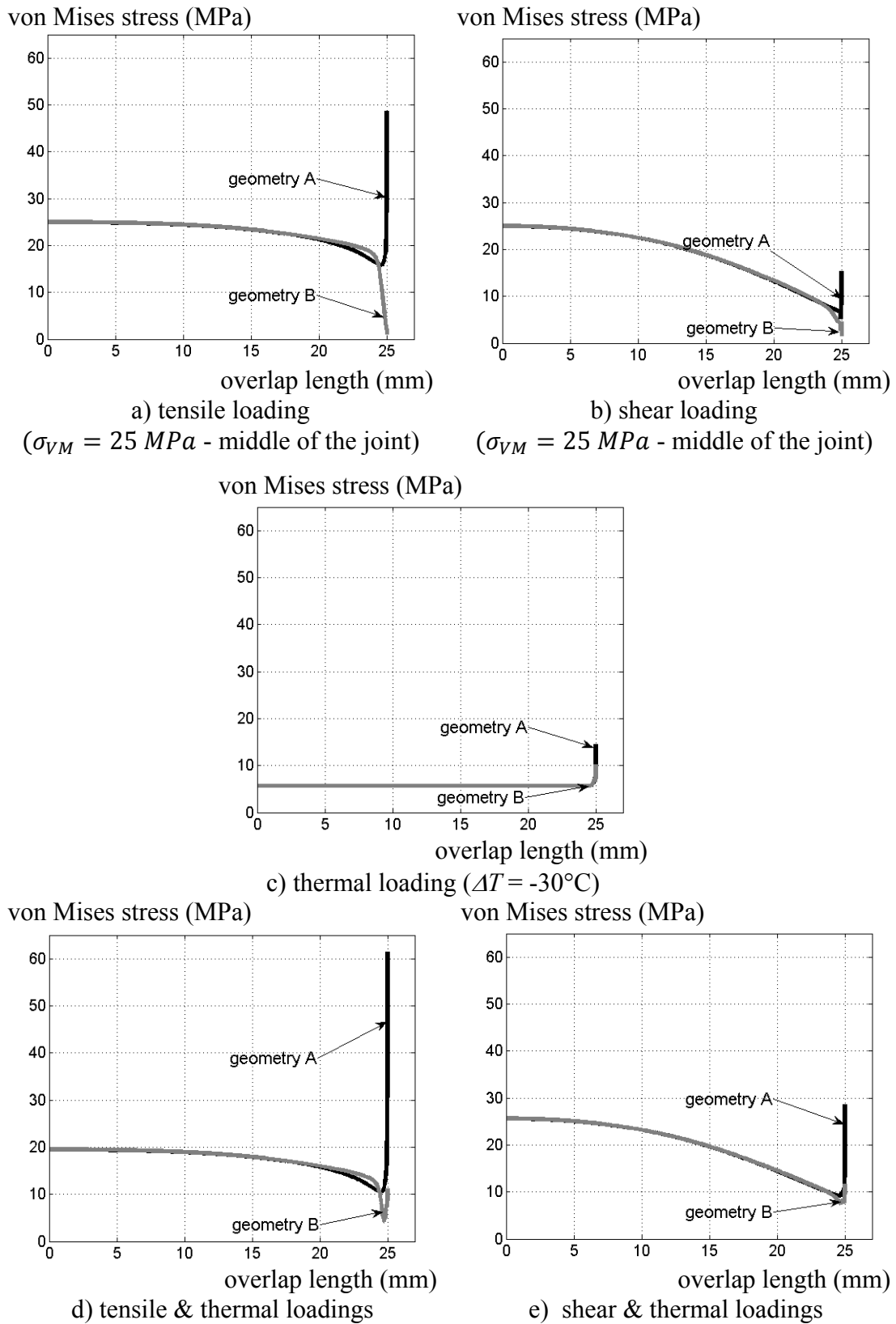


Figure 4: Thermo-mechanical stress in the adhesive under tensile and shear loadings.

For this analysis, using 2D finite element simulations [16] under elastic assumption of the components, one assumes that no residual stress exists at room temperature. Results are presented for two geometries of the bonded specimens used with the modified Arcan device (Figure 3). The first geometry is associated with straight substrates and straight edge of the free edges of the adhesive and the second geometry represents the bonded specimens proposed for the experimental tests; they are characterised by the use of beaks on the substrates and a cleaning of the free edges of the adhesive in order to obtain a significant reduction in the stress concentrations in the adhesive under mechanical loads [11]. Geometries are defined with the following parameters: $L = 50$ mm, $HI = 20$ mm, $\alpha = 30^\circ$, $h = 0.1$ mm, $d = 0.5$ mm, $r = 0.1$ mm and $e = 0.2$ mm.

Under mechanical loads, the maximum value of the stress in the adhesive is obtained close to the substrate-adhesive interface for geometry A (straight substrates and straight free edges of the adhesive), and within the adhesive for geometry B (substrates with beaks and cleaned edges of the free edges of the adhesive) [11]. Thus, in order to simplify the presentation, we have chosen to plot the maximum value of the von Mises stress through the joint thickness for a given point of the overlap length, with respect to the overlap length x . For the mechanical load, displacements (in the x and y direction) are prescribed on the upper and lower lines of the model presented in Figure 3, as the Arcan support is nearly rigid with respect to the adhesive rigidity. Figures 4a and 4b present the evolution of the maximum value of the equivalent von Mises stress with respect to the overlap for geometries A and B. The mechanical load has been chosen in order to obtain a value of the equivalent von Mises stress of 25 MPa in the middle of the joint in order to analyse results under tensile and shear loads. It can be noted that geometry B allows a large reduction in the stress concentrations close to the free edges of the adhesive [11]. For the thermal load, a variation of $\Delta T = -30^\circ\text{C}$ (test at -10°C) is prescribed (analysis between room temperature, 20°C , and at -10°C). Figure 4c underlines that such a loading leads to a quite low stress state in the adhesive, but for geometry A, larger stress concentrations can be noted than for geometry B. For the thermo-mechanical loads, Figures 4d and 4e present the stress state for a variation in temperature of $\Delta T = -30^\circ\text{C}$ followed by the previous mechanical load. They represent tests under tensile and shear loads at -10°C . The superposition of the thermal load to the mechanical load leads to an increase in the stress concentrations close to the free edges of the adhesive (geometry A). For geometry B, an increase in the mechanical load leads to a decrease in the stress state close to the free edges of the adhesive with respect to the stress state in the middle of the joint; thus it leads to a reduction in the stress concentrations. On the other hand, it has been shown that for tests with quite large stress concentration, cracks can appear quickly at the two edges of the joint, close to the adhesive-substrate interfaces [11, 17], and thus can lead to an incorrect analysis of the behaviour of the adhesive. Therefore, for geometries characterized with large stress concentrations under mechanical loads (such as geometry A) a decrease in the temperature of the mechanical test is associated with an increase in the stress concentrations and thus to earlier crack initiation. It can be noted that the use of straight free edges of the adhesive strongly increases the stress concentrations in the adhesive [11]. Moreover, such simulations can require more refined meshes in

order to obtain accurate numerical results [18]. The use of beaks and of cleaned free edges of the adhesive allows to strongly limit the stress state close to the free edges of the joint. It allows to reach the elastic limit first in the middle of the joint, and thus to analyse accurately the non linear behaviour of the adhesive in an assembly for a large range of temperatures and for a large range of proportional tensile/compression-shear loads (modified Arcan device).

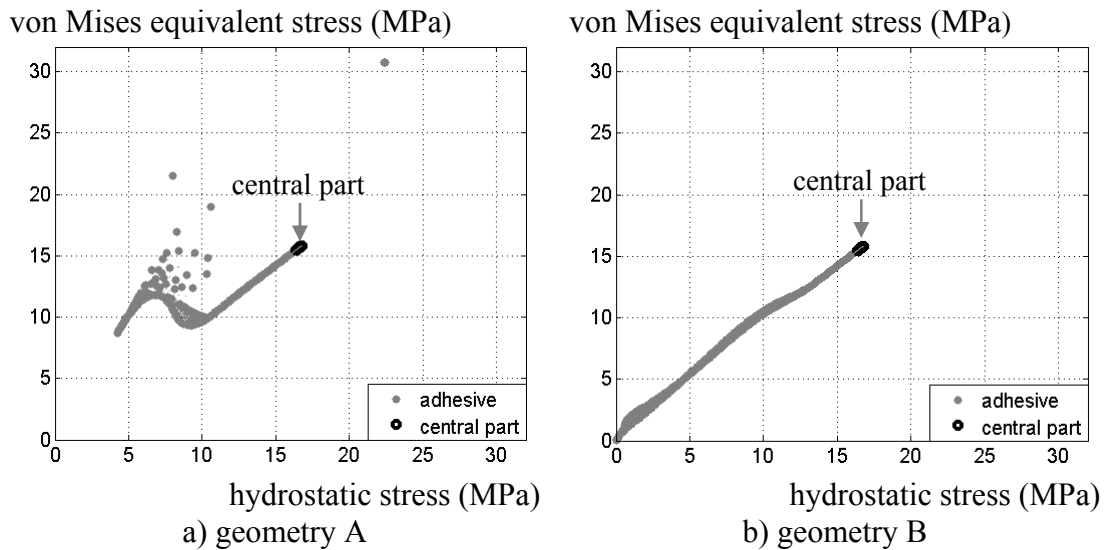


Figure 5: Stress state in the adhesive under tensile load (average peel stress, σ_{yy} , of 25 MPa) in the hydrostatic stress - von Mises equivalent stress diagram.

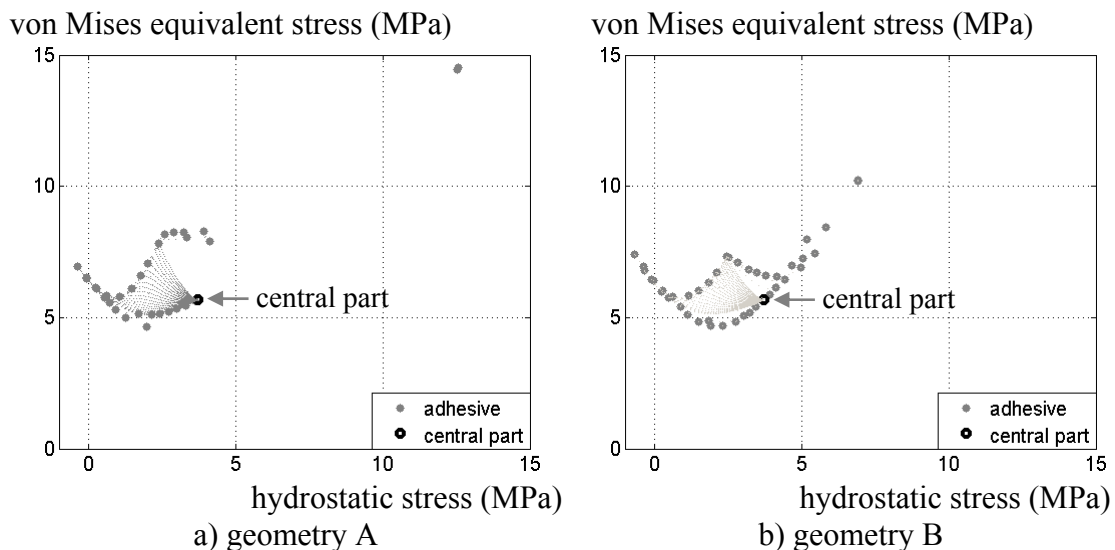


Figure 6: Stress state in the adhesive under thermal load ($\Delta T = -30^\circ\text{C}$) in the hydrostatic stress - von Mises equivalent stress diagram.

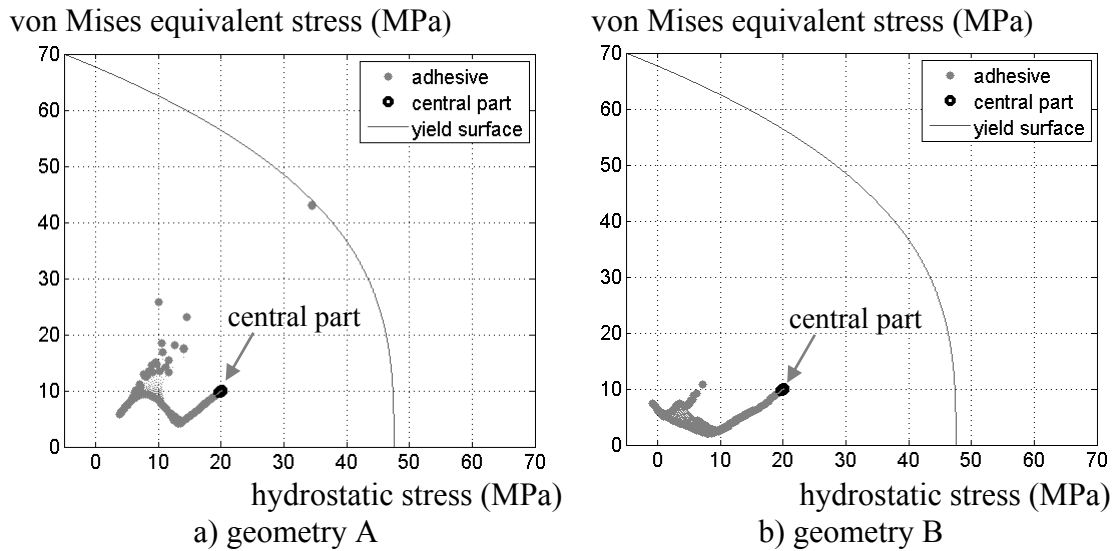


Figure 7: Stress state in the adhesive under thermal load ($\Delta T = -30^{\circ}\text{C}$) and tensile load (average peel stress, σ_{yy} , of 24.5 MPa) in the hydrostatic stress - von Mises equivalent stress diagram.

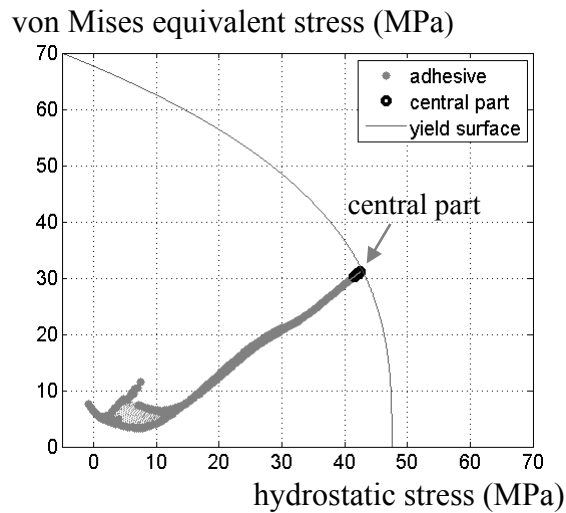


Figure 8: Stress state in the adhesive under thermal load ($\Delta T = -30^{\circ}\text{C}$) and tensile load (average peel stress, σ_{yy} , of 57.8 MPa) in the hydrostatic stress - von Mises equivalent stress diagram for geometry B.

Figure 4 underlines that stress concentrations are more important under tensile loadings; thus this case is analysed in the following, using the representation of the stress state in the hydrostatic stress - von Mises equivalent stress diagram.

Figure 5 presents the stress state in the whole adhesive under a tensile loading associated with an average peel stress (σ_{yy}) of 25 MPa for geometries A and B (Figure 3). It can be noticed that the stress states in the middle part of the joint ($x \in [-5 \text{ mm}, 5 \text{ mm}]$), represented using black marks, are similar for the two geometries

as the stress concentrations are only observed close to the free edges of the adhesive. This diagram presents the stress state for each element of the mesh used in the computation.

Figure 6 presents the stress state in the whole adhesive under a thermal loading associated with a variation of the temperature of $\Delta T = 30$ °C for geometries A and B. As presented in Figure 4, it can be noted that for both geometries, the maximum values of the stress state are obtained close to the free edges of the adhesive (not in the middle part of the joint). But, the stress state is lower for geometry B than for geometry A.

Figure 7 presents the stress state in the whole adhesive under a tensile loading associated with an average peel stress (σ_{yy}) of 24.5 MPa and a thermal load associated with a variation of the temperature of $\Delta T = 30$ °C, for geometries A and B. Moreover, in Figure 7 the elastic limit for an experimental test at -10°C of the adhesive is plotted. For such thermo-mechanical loading the elastic limit is reached in adhesive in the case of geometry A, close to the free edges. One again, it can be noticed that the stress states in the middle part of the joint are identical for the two geometries.

Figure 8 presents the stress state in the whole adhesive under a tensile loading associated with an average peel stress (σ_{yy}) of 57.8 MPa and a thermal load associated with a variation of the temperature of $\Delta T = 30$ °C, for geometry B. For such thermo-mechanical loading the elastic limit is reached in adhesive in the case of geometry B, in the middle of the joint.

Thus, for such thermo-mechanical loading, under elastic assumption, the maximum transmitted tensile load by geometry B is more than twice higher than for geometry A. Same results can be obtained for single lap shear type specimens as for geometry A, as large stress concentrations can be obtained for such specimens [19]. These results underline the strong influence of stress concentrations in bonded assemblies on the experimental analysis of the mechanical behaviour of an adhesive in an assembly. Therefore the use of geometries of bonded specimens which strongly limit stress concentrations are necessary to accurately analyse the non-linear behaviour of an adhesive.

5 Influence of temperature on the adhesive Behaviour

In order to underline the possibilities of the proposed modified Arcan device, with the specific design of the bonded assemblies, to analyze the influence of the temperature on the mechanical behavior of an adhesive in assembly under a large range of mechanical loadings, various experimental tests are presented in the following.

Tests were made with a displacement rate of the crosshead of the tensile testing machine of 0.5 mm/minute. Four loading paths were analysed using the modified Arcan device (Figure 1): tensile ($\gamma = 0^\circ$), tensile-shear ($\gamma = 45^\circ$), shear ($\gamma = 90^\circ$) and compression-shear ($\gamma = 135^\circ$). Moreover different temperatures were taken into account starting from room temperature: 20 °C, 0 °C, -20 °C, -40 °C and -60 °C.

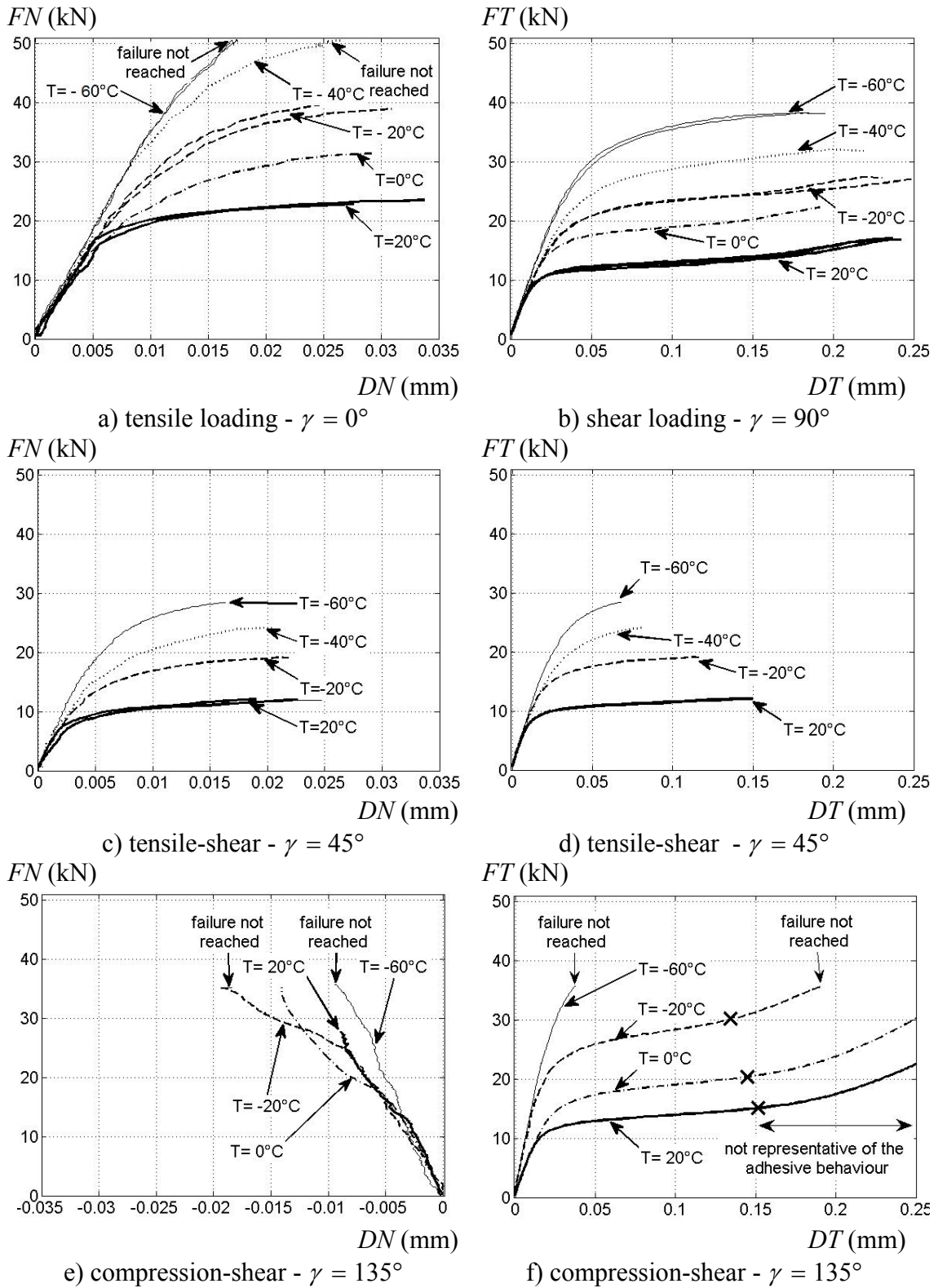


Figure 9: Influence of the temperature on the mechanical behaviour of the adhesive in the load-relative displacement diagram for different monotonic radial loads.

The experimental results are presented in the load-displacement diagrams in Figure 9. The results present the mechanical load transmitted by the bonded assembly for a given temperature. A more precise analysis requires the stress state associated with the thermal loading to be taken into account; such a study is not presented herein.

For compression-shear loads ($\gamma = 135^\circ$), the failure load is not easy to determine. In fact, for such tests, in the non-linear phase of the adhesive behaviour, the change in the slope of the response in the load-deformation diagram can be associated with the failure of the joint. These points are represented using the following marks “x” in Figure 9f. Moreover, for such compression-shear loads ($\gamma = 135^\circ$) the scatter in the experimental results is higher for the normal displacement (Figure 9e), mainly associated with the view-glass of the thermal chamber. However, it is important to underline that under such loadings, the tangential displacement is much higher than the normal displacement (Figure 9e-f).

The scatter in the experimental results is quite low for the different temperatures. Similar low scatter in the results has been obtained with such a modified Arcan device designed to limit stress concentrations significantly [11, 12]. Moreover, a diminution in the temperature, leads to a low reduction in the deformation at failure of the adhesive and to a large increase in the elastic limit and in the failure stress of the adhesive for the different compression/tensile-shear loads.

The last property, explains that for some tests, the failure has not been reached as the maximum transmitted load has been limited to 50 kN in order to prevent permanent deformation of the Arcan device and of the loading pins, as they have not been designed for such heavy loads

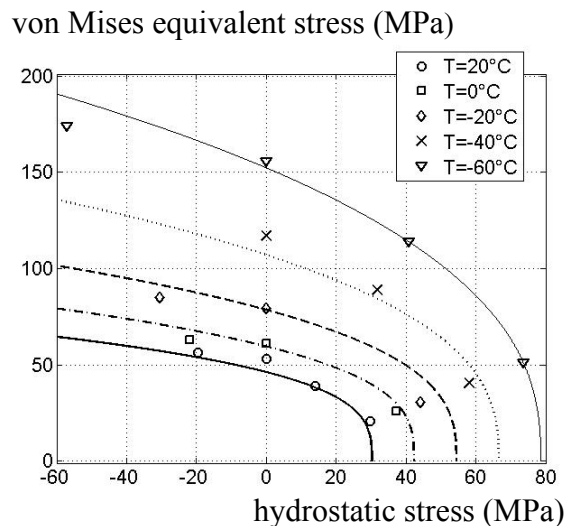


Figure 10: Modelling of the temperature-dependent elastic limit of the adhesive in the hydrostatic pressure - von Mises stress diagram.

Figure 10 presents, for the elastic limit, a comparison between the experimental results and the numerical model (presented in section 3) for the different studied temperatures in the hydrostatic pressure-von Mises stress diagram.

A good representation of the experimental results is obtained using such type of model for the elastic limit.

6 Conclusions

In this paper it has been shown, starting from 2D numerical simulations, that the use of substrates with beaks allows to strongly limit the stress concentrations for bonded assemblies under thermo-mechanical loads. The influence of the service temperature on the stress concentrations has been analysed in order to define the requirements of the bonded specimens in order to obtain reliable experimental tests. Such thermo-mechanical loads can lead to complex history path in the von Mises equivalent stress – hydrostatic stress plane which is often used to describe the temperature dependent elastic limit of an adhesive. Therefore, experimental results under a large range of mechanical loads are required to develop accurate numerical models. Some experimental results, for a temperature range between 20 °C and -60 °C using a modified Arcan device designed to strongly limit stress concentrations, are presented in order to validate the proposed numerical studies. The experimental results underline that a diminution in the temperature leads, on the one hand to a low reduction in the deformation at failure of the adhesive; and on the other hand, to a large increase in the elastic limit and of the failure stress of the adhesive for the different compression/tensile-shear loads.

As the stress state in an adhesive joint with the modified Arcan device is quite complex, inverse identification techniques using three-dimensional finite element models are necessary to analyse the experimental results accurately. Thus, the proposed experimental strategy can be interesting to analyse the temperature-dependent visco-plastic behaviour of an adhesive in an assembly under various thermo-mechanical loads. Moreover, the influence of residual stresses, associated with the curing process of the adhesive, has also to be analysed [20].

References

- [1] R.D. Adams, Adhesive bonding: Science, technology and applications, Woodhead Publishing Limited, 2005.
- [2] L.F.M. da Silva and A. Öchsner, Modeling of adhesive bonded joints, Springer, Berlin, 2008.
- [3] L.F.M. da Silva, A. Öchsner and R.D. Adams, Handbook of Adhesion Technology, Springer, Heidelberg, 2011.
- [4] Z.Q. Qian, On the evaluation of wedge stress intensity factor of bi-material joints with surface tractions, Computers & Structures, 79, 53-64, 2001.
- [5] D. Leguillon and E. Sanchez-Palencia, Computation of singular solutions in elliptic problems and elasticity, Editions Masson, Paris, 1987.
- [6] W.K. Chiu, P.D. Chalkley, R. Jones, Effects of temperature on the shear stress-strain behavior of structural adhesive, Computers & Structures, 53, 483-89, 1994.

- [7] M.K. Apalak, R. Gunes, On non-linear thermal stresses in an adhesively bonded single lap joint, *Computers & Structures*, 80, 85-98, 2002.
- [8] L.F.M. da Silva, R.D. Adams, Stress-free temperature in a mixed-adhesive joint, *Journal of Adhesion Science and Technology*, 20, 1705–1726, 2006.
- [9] L.D.R. Grant, R.D. Adams, L.F.M. da Silva, Effect of the temperature on the strength of adhesively bonded single lap and T joints for the automotive industry, *International Journal of Adhesion & Adhesives*, 29, 535–542, 2009.
- [10] R. Mahnken, M. Schlimmer, Simulation of strength difference in elasto-plasticity for adhesive materials, *Int. J. Numerical Methods in Engineering*, 63, 1461-1477, 2005.
- [11] J.Y. Cognard, Numerical analysis of edge effects in adhesively-bonded assemblies. Application to the determination of the adhesive behaviour, *Computers & Structures*, 86, 1704-1717, 2008.
- [12] J.Y. Cognard, P. Davies, L. Sohier, R. Créac'hcadec, “A study of the non-linear behavior of adhesively-bonded composite assemblies”, *Composite Structures*, 76, 34-46, 2006.
- [13] J.Y. Cognard, R. Créac'hcadec, L.F.M. da Silva, F.G. Teixeira, P. Davies, M. Peleau, Experimental analysis of the influence of hydrostatic stress on the behaviour of an adhesive using a pressure vessel, *Journal of Adhesion*, 87, 804-825, 2011.
- [14] Gom documentation, www.gom.com.
- [15] C. Badulescu, J.Y. Cognard, R. Créac'hcadec, P. Vedrine, Analysis of the temperature-dependent behaviour of a ductile adhesive under monotonic tensile/compression-shear loads, *International Journal of Adhesion and Adhesives* (under press).
- [16] Abaqus documentation, Version 6.6. Simulia, 2007.
- [17] G. Dean, L. Crocker, B. Read, L. Wright, Prediction of deformation and failure of rubber-toughened adhesive joints. *International Journal of Adhesion and Adhesives*, 24, 295-306, 2004.
- [18] J.Y. Cognard, L. Sohier, R. Créac'hcadec, F. Lavelle, N. Lidon, Influence of the geometry of coaxial adhesive joints on the transmitted load under tensile and compression loads. *International Journal of Adhesion and Adhesives* (DOI:10.1016/j.ijadhadh.2012.01.013), 2012.
- [19] J.Y. Cognard, R. Creac'hcadec, L. Sohier, P. Davies, Analysis of the non linear behaviour of adhesives in bonded assemblies. Comparison of TAST and ARCAN tests, *International Journal of Adhesion & Adhesives*, 28, 393-404, 2008.
- [20] Y. Yu, I.A. Ashcroft, G. Swallowe, An experimental investigation of residual stresses in an epoxy–steel laminate, *International Journal of Adhesion & Adhesives*, 26, 511-519, 2006